ELSEVIER

Carbohydrate Polymers 46 (2001) 383–391

Carbohydrate Polymers

www.elsevier.com/locate/carbpol

Interpenetrating network formation in agarose–sodium gellan gel composites

E. Amici, A.H. Clark*, V. Normand, N.B. Johnson

Unilever Research Colworth, Colworth House, Sharnbrook, Bedford MK44 1LQ, UK

Received 3 July 2000; revised 26 September 2000; accepted 13 November 2000

Abstract

Aqueous cold-set gels from mixtures of agarose and sodium gellan have been characterised structurally and mechanically using optical and electron microscopy, turbidity measurements, differential scanning calorimetry, mechanical spectroscopy and compression testing. Consistent with expectations for charged–uncharged polymer combinations at low ionic strength there is no liquid–liquid demixing in sols prior to gelation, and although transmission electron microscopy reveals heterogeneities in gel microstructures at the higher polymer concentrations, these are small in extent, and are unlikely to arise from normal segregative demixing. Overall, 'molecularly' interpenetrating networks (IPNs) are indicated, in which the gellan and agarose architectures pass through one another on a distance scale comparable to their pore sizes. At concentrations greater than 2% w/w gellan, where gellan is the first gelling species, and when the agarose concentration is greater than 0.5% w/w, the composite modulus falls below that expected for the agarose alone. At 0.5% w/w agarose, on the other hand, modulus contributions from the components are much closer to additive. These findings are reflected in the results of large deformation compression testing where breaking stresses show similar trends. © 2001 Elsevier Science Ltd. All rights reserved.

Keywords: Agarose; Gellan; Interpenetrating networks; Compression testing; Mechanical spectroscopy; Confocal microscopy; Electron microscopy; Turbidity; Scanning calorimetry

1. Introduction

Mixed aqueous biopolymer systems, solutions and gels, have been extensively studied over the last few years (Kasapis, Morris, Norton & Clark, 1993; Lundin, Norton, Foster, Williams, Hermansson & Bergstrom, 2000; Michon, Cuvelier, Launay & Parker, 1996; Tolstoguzov, 1995; Tromp, Rennie & Jones, 1995; Walkenstrom & Hermansson, 1996) not least because of their increasing importance in industrial applications. In the majority of examples considered, some level of demixing and phase separation was observed prior to, or during, the gelling event. This was assumed to be largely a consequence of the intrinsic tendency of polymer solutions to have reduced mixing entropy in comparison with solutions of simpler molecules. Indeed, the effect has been well documented in work extending from the original Flory–Huggins treatment of the phenomenon (Flory, 1953) to more recent experimental (Medin & Janson, 1993) and theoretical studies (Clark, 2000; Picullel, Bergfeldt & Nilsson, 1995; Picullel, Iliopoulos, Linse, Nilsson, Turquois, Viebke et al., 1994). Homogeneous mixed systems seem only to arise in situations where some form of specific attraction between the polymer components occurs, i.e. some form of coupled or synergistic network forms, as discussed in detail in a recent review (Morris, 1995).

Other types of homogeneous mixed gel may be possible, however. For example, in a classification of mixed gel types published some time ago (Morris, 1986), a category of system was suggested in which one biopolymer network passed through another at what amounted to the molecular distance scale, or at least a distance scale very close to this. Such networks might be called interpenetrating (i.e. IPNs), but they should be distinguished from more genuinely phase-separated microstructures involving interpenetrating phases or microphases, i.e. bicontinuous phase-separated systems. A greater degree of homogeneity seems to be implied by the more intimate type of IPN suggested. The question now is, do examples of this type of structure actually exist? So far no really clear-cut case seems to have been reported.

If they exist at all, such intimate IPNs are clearly not common, and it is expected that they will require rather special conditions and circumstances for their formation. Either the driving force for polymer–polymer demixing should remain low (or preferably zero) during molecular

* Corresponding author. Fax: +44-1234-22-2757.
E-mail address: allan.clark@unilever.com (A.H. Clark).

0144-8617/01/$ - see front matter © 2001 Elsevier Science Ltd. All rights reserved.
PII: S0144-8617(00)00342-8

aggregation and network building, or the first gelling component should aggregate so rapidly and uniformly, that the second gelling system is forced to aggregate within the pores of the first. The first condition is a thermodynamic one, the second kinetic (i.e. kinetic trapping is implied). In practice, some combination of these effects may be required, such as a lack of a thermodynamic tendency to demix, at least in the earliest stages of aggregation, coupled to rapid and homogeneous network building by at least one of the components.

The present paper seeks to produce and characterise mixed polysaccharide gels of this 'molecularly interpenetrating' type, where the term 'molecular' is used rather loosely to extend in distance scale to the bundles of molecular helices comprising the fibrous strands of the networks involved. In the present work the biopolymer combination selected was agarose and gellan. For these polysaccharides, at low ionic strength, the thermodynamic tendency to demix is likely to be greatly reduced by the well-known counterion entropy effect (Picullel et al., 1994, 1995). Also, polysaccharides such as these undergo rapid conformational changes and aggregation events when they gel and, as individual polymers, form reasonably homogeneous gel networks. Conditions for molecular IPN formation are therefore likely to be optimal for this polymer pair.

In the work described here, mixtures of agarose and sodium gellan were cooled from what were identified as homogeneous sol states and the resulting gels (and the kinetics of their formation) studied by differential scanning calorimetry (DSC), small and large-deformation mechanical measurements, turbidity measurements, and optical and electron microscopy. The agarose used was chosen to be as uncharged as possible (i.e. to be agarose rather than food grade agar) and the gellan was purified to be in the sodium salt form rather than in the less well-defined commercial mixed ion form. In this way it was possible to start with a simple charged–uncharged polymer combination which theory suggests should greatly resist demixing under conditions of limited ionic strength (no additional salt was added in the present investigations).

2. Materials and methods

2.1. Agarose

The agarose was obtained from Sigma and was Type 1-A, lot 56H1046 (ash $<0.5\%$, sulphate $<0.2\%$). The weight average molar mass (1.7×10^5 g/mol) was determined by high performance size exclusion chromatography and multi-angle laser light scattering.

2.2. Gellan

The starting material Kelcogel F was supplied by Kelco. This mixed ion form was dissolved in 1% aqueous 2-propanol and precipitated as the acid form using 0.1 N HCl. The washed precipitate was dispersed in water and titrated against 2 N NaOH until complete dissolution and neutralisation. The solution was dialysed initially against 0.05 M EDTA and then exhaustively against distilled water. The purified gellan was recovered by freeze-drying. Size exclusion chromatography and multi-angle laser light scattering provided a weight average molar mass of 1.1×10^5 g/mol for the purified material. This was shown to contain 2.83% w/w sodium and only negligible amounts of potassium and calcium.

2.3. Solutions

These were prepared by accurate weighing of components at ambient followed by heating at boiling point for 20 min with stirring to fully dissolve and disorder the polysaccharides. In general, a protocol was adopted in which several agarose concentrations were considered (e.g. 0.5, 1.0 and 2.0% w/w) and increasing levels of gellan added up to 5% w/w.

2.4. Differential scanning calorimetry (DSC)

Measurements were performed using a Setaram micro-DSC II batch and flow calorimeter. Sample pans were filled with approximately 800 mg of solution, the precise figure obtained by accurately weighing. Water-filled reference pans were adjusted to weigh within 20 μg of the samples. Prior to measurement, systems were taken to high temperature to eliminate thermal history effects, and cooling and heating scans performed at 1.0°C/min. Onset and peak temperatures and enthalpies of transitions were calculated by computer using baseline subtraction and integration routines.

2.5. Mechanical spectroscopy

Measurements of storage and loss shear moduli G' and G'' were performed using a Carrimed CSL 500 stress-controlled rheometer. A coaxial cylinder geometry was employed (gap 3 mm). The hot solutions were mounted on a layer of perfluorodecalin and covered with Silicone oil to minimise water loss. Experiments were performed at 1 Hz and 0.5% strain and, except where indicated, solutions were cooled at 1°C/min from 70 to 10°C, and held at 10°C for 5 h.

2.6. Large-deformation compression tests

Compressive strengths for the gels were measured under uniaxial compression on an Instron Universal Testing Machine Model 4502 using a parallel plate geometry. Test parameters were load cell 0.1 kN, and cross-head speed 50 mm/min. Gel samples were prepared in cylindrical moulds (12.2 mm height, 12.5 mm diameter) by cooling hot solutions at ambient; then overnight at 10°C. Between 6 and 10 replicates were tested for each composition. Samples were self-lubricating due to water exudation during compression. Corrected true stress was calculated as $\sigma =$

FH/A_oH_o, where H is the specimen height, H_o the original height, A_o the original cross-sectional area, and F the applied load. The corrected true strain (Hencky strain) was calculated as $\epsilon = \ln(H/H_o)$. Compressive elastic moduli were calculated from data in the initial linear regions of the stress–strain curves.

2.7. Turbidimetry

Measurements were performed using a Shimadzu UV-2101PC UV–Vis scanning spectrophotometer in the range 400–800 nm and with a path length of 1 cm. Solutions and reference samples (water) were introduced into pre-heated quartz cuvettes at 70°C, allowed to equilibrate, then cooled to 10°C at 1°C/min. Temperature was controlled using a programmable circulating water bath.

2.8. Confocal microscopy

The confocal instrument was a Bio-Rad MRC 600 confocal scanning laser microscope with a laser excitation at 488 nm. Hot solutions (with added Rhodamine-B) were placed on preheated slides and mounted on the microscope stage held at 70°C. The stage was cooled to 20°C at 1°C/min and micrographs recorded. Some work using conventional phase contrast optical microscopy was also performed.

2.9. Transmission electron microscopy

Gel samples produced by cooling hot solutions from 70 to 10°C at 1.0°C/min were cut into 1 mm cubes and fixed by immersion in 0.05% ruthenium tetroxide (2 h at ambient). The samples were washed and progressively dehydrated using a series of ethanol solutions (50, 70, 90 and 100%). The dehydrated samples were then resin embedded over a period of eight days followed by resin polymerisation at 55°C. Samples were sectioned (Ultracut-E microtome) and stained using anti-agarose antibody/gold conjugate and uranyl acetate and lead citrate. Micrographs were obtained using a JEOL 1220 transmission electron microscope.

3. Results and discussion

3.1. DSC measurements

This approach allowed details of the molecular ordering transitions (coil-to-helix) underlying network formation to be characterised both for the pure components and for their mixtures. Experiments were confined to samples containing 1% w/w agarose and 1–5% w/w added gellan. Results (cooling and heating curves) for the pure 1% agarose system appear in Fig. 1. This shows a sharp exotherm below 40°C, on cooling, with a much broader and higher temperature endotherm being measured on heating. Hysteresis behaviour of this kind is expected for agarose (and for a number of other gelling polysaccharides), and has its origin in aggregation of the helices formed initially. In such a situation,

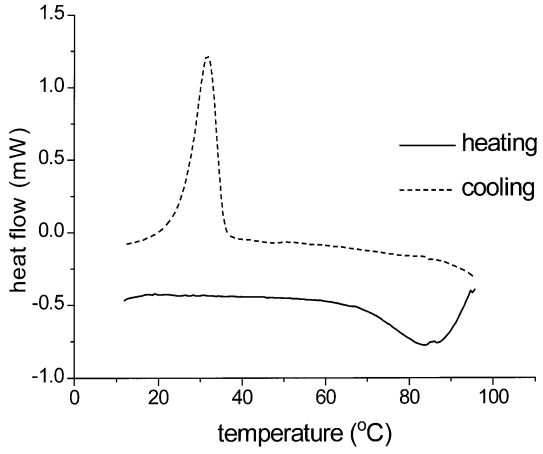

Fig. 1. DSC cooling and heating scans for a 1% w/w agarose system. Scan rate is 1°C/min.

melting is determined by helix–helix interactions, while setting requires preliminary molecular ordering, and only occurs below the coil–agarose double helix conformational transition temperature.

Corresponding cooling and heating DSC results appear for the gellan component at five concentrations (1–5% w/w) in Fig. 2. The cooling exotherms are significantly concentration dependent as is expected for a polyelectrolyte at low ionic strength. When compared to these, the melting endotherms also exhibit hysteresis, particularly at gellan concentrations above 2% w/w. Again, as for agarose, this indicates aggregation of the ordered conformation in the

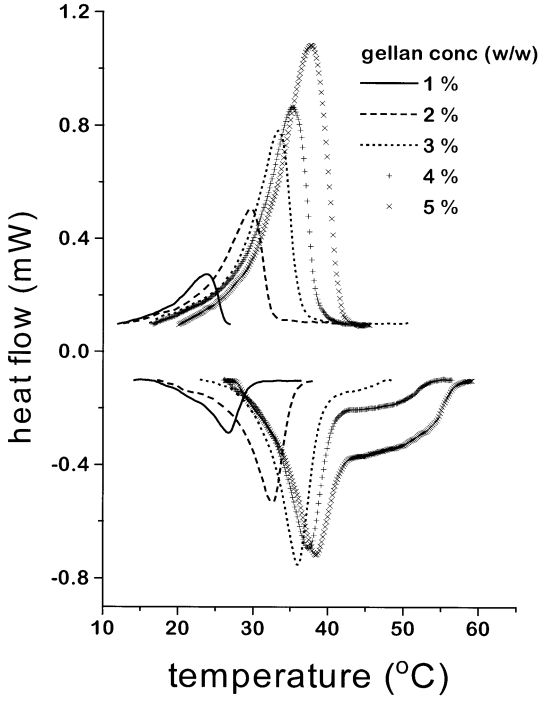

Fig. 2. DSC cooling (top) and heating (bottom) scans for gellan at different concentrations. Scan rate is 1°C/min.

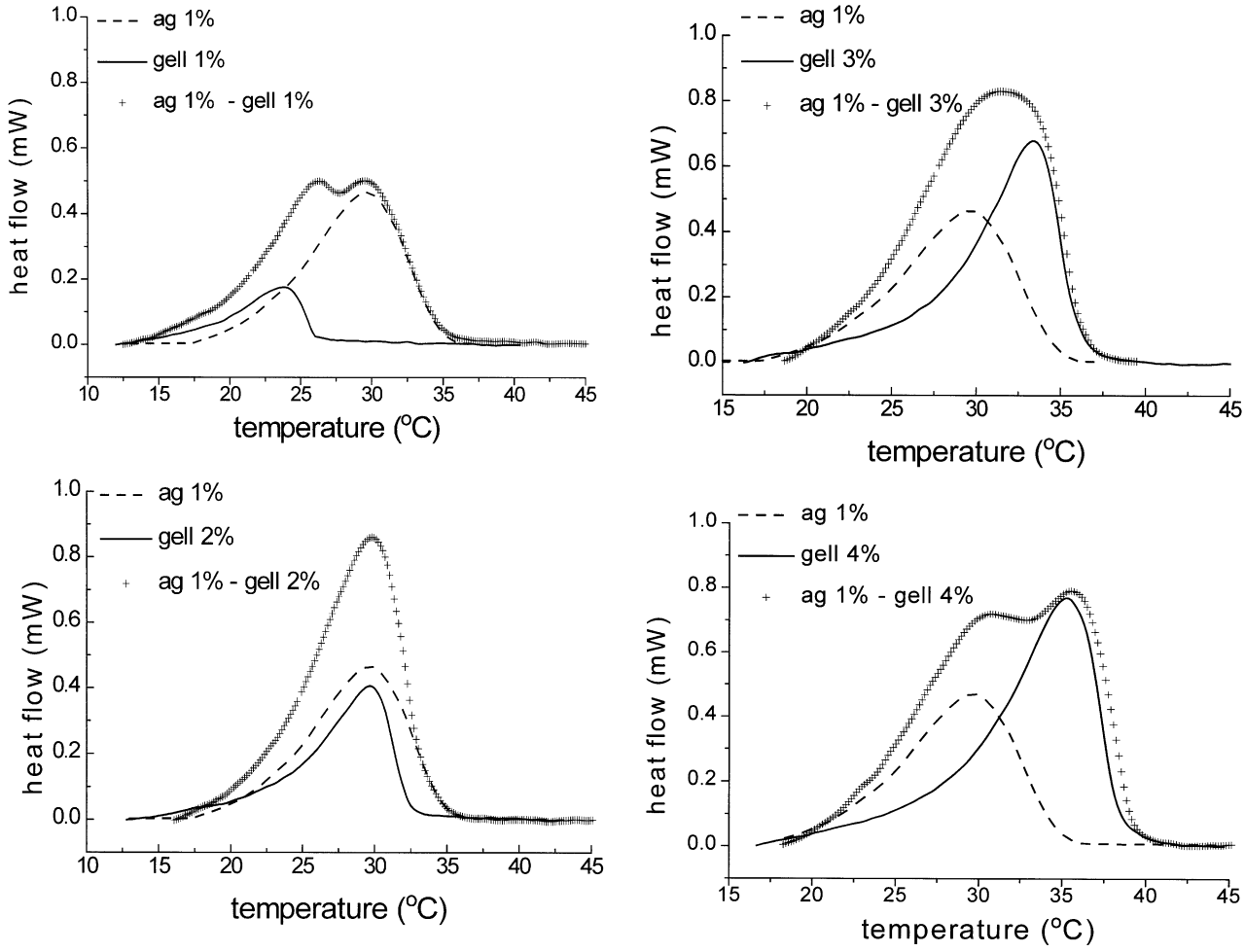

Fig. 3. DSC cooling scans of agarose (1% w/w), gellan (1–4% w/w) and their mixtures. Scan rate is 1°C/min.

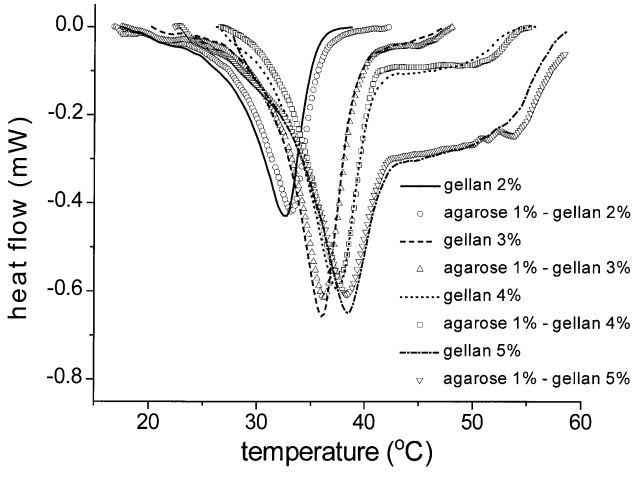

Fig. 4. DSC heating scans of gellan (2–5% w/w) and its mixtures with 1.0% w/w agarose. Scan rate is 1°C/min.

more concentrated solutions. The effect is much smaller for sodium gellan at low ionic strength, however, with only a growing shoulder appearing in the melting transition peaks.

DSC results for the mixtures are compared to the pure component behaviours in Figs. 3 and 4. From Fig. 3, which shows cooling results for four gellan concentrations and a fixed 1% level of agarose, two things are evident: (1) as can be verified quantitatively, the mixture exotherms can be represented as simple sums of the contributions expected for the pure components; and (2) there is a switch-over at roughly 2% w/w gellan content, in terms of which polymer orders first as the temperature falls. Below this level of gellan, the agarose first forms helices, while the reverse is true as the gellan concentration increases.

The melting endotherms for pure gellan systems and for the mixtures with agarose, appear in Fig. 4, which shows only the lower temperature response due to the gellan (i.e. the higher temperature, and broader, agarose melting contribution is not included). Evidently, the gellan melting profiles, when in mixture form, closely match those from gellan alone at the same concentration. It seems clear that helix formation, and indeed accompanying processes of

aggregation, are largely unperturbed in the mixtures, i.e. one component has little influence on the other.

3.2. Mechanical spectroscopy

Cure curves for the individual agarose and gellan components were readily obtained. For agarose, these had the usual form of a rapid rise in the shear modulus at some specific point during cooling, followed by an abrupt plateauing off at longer times. For the purified sodium gellan the critical gelation concentration was found to be rather high (2% w/w $< Co <$ 3% w/w) and the cure behaviour was less conventional. Data for a cooled 4% w/w solution appear in Fig. 5 and here, not only is the long-time shear modulus obtained rather low, but it is also made uncertain by what are evidently slippage effects occurring as the temperature fall is halted at 10°C. This poor gelling behaviour exhibited by the sodium salt of gellan when gelled at low ionic strength restricted possibilities for modelling the composite modulus data (see later discussion) but it did not prohibit the main features of the phenomenon from being established. In practice, for gellan, maximum moduli extracted from cure curves were used as best long-time estimates.

Cure curve results for the mixtures were obtained both in situations where the agarose gelled first (Fig. 6 — agarose 1%, gellan 2%) and the gellan was below its critical concentration; and in situations where the gellan gelled first (Fig. 7 — agarose 1%, gellan 5%). Fig. 6 shows that the influence of gellan is very minor in the agarose dominated systems, the modulus–temperature cure curve behaviour being almost completely ascribable to the gelling of the agarose. Fig. 7, on the other hand, shows an initial shoulder in the cure data corresponding to a preliminary gellan gelling event. This is followed by a later and quite strong agarose contribution.

Results obtained for final long-term G' moduli from cure curves for a range of mixture compositions and for two levels of agarose (0.5 and 1.0% w/w) are summarised in Fig. 8. The peak G' values for gellan alone (concentration range 3 to 5% w/w) are included for comparison. At 1% agarose there is quite clearly a fall in G' at the point where the gellan gels first, i.e. above the gellan critical concentration. Some recovery of the modulus is indicated as the gellan concentration is increased, but it still only approaches the pure agarose value. Data for a series containing 2% agarose (not shown) showed a similar effect, though in this case the dip in G' was much less pronounced. Clearly, for the 1% agarose level, and above, while the system has a much higher modulus than would be expected for the gellan alone (see pure gellan values), simple additivity of moduli, such as might be proposed for an IPN situation, does not hold even approximately. The agarose contribution is somehow reduced and inhibited when it gels second. At the lowest agarose content (0.5% w/w), however, Fig. 8 shows that the composite modulus can almost be represented as a sum of contributions from the pure components, increasing as it does over the pure agarose value as the gellan content increases. In this case the composite modulus is actually somewhat higher than would be predicted on the basis of simple summation (but note comments earlier about limited reliability of the pure gellan modulus estimates).

A final point worth noting is that for the 1% agarose/4% gellan system, experiments conducted under both low (0.005°C/min) and rapid cooling (sudden quench) conditions produced similar results, suggesting thermodynamic rather than kinetic inhibition of demixing in these systems. Kinetic trapping, if critical, would presumably lead to rather different microstructures over the range of cooling rates studied. Electron micrographs of the gels produced under these different regimes were also essentially unaltered in relation to that for the structure obtained at 1°C/min (see a later section).

3.3. Turbidity studies

Changes in turbidity during gelling appear in Fig. 9 for 1.0% w/w agarose and its mixtures with gellan in the range 3

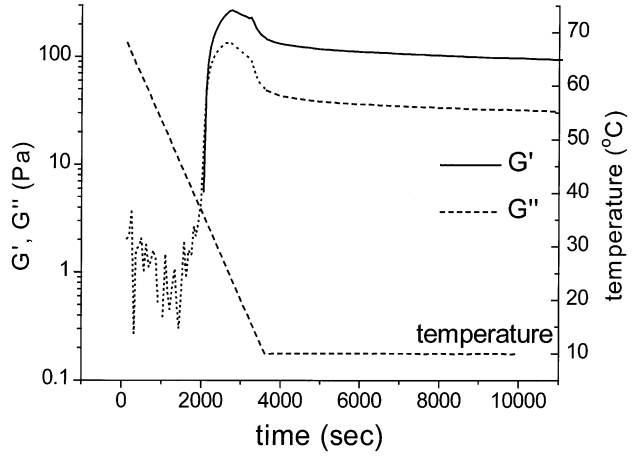

Fig. 5. Variation of G' and G'' (1 Hz, 0.5% strain) with time and temperature during gelation of 4% w/w gellan. Solutions were cooled from 70°C to 10°C at 1°C/min and held at 10°C for five hours.

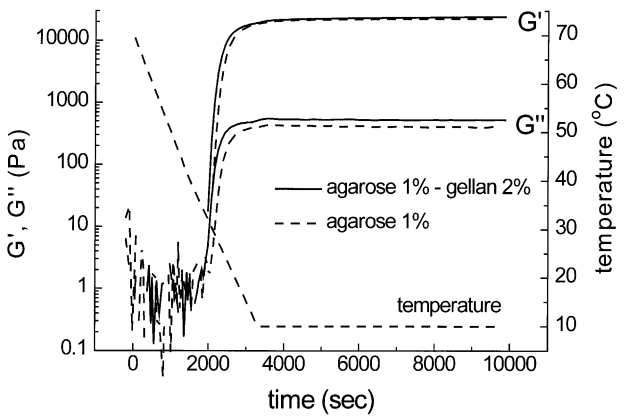

Fig. 6. G' and G'' cure curves for the agarose 1% w/w–gellan 2% w/w system are compared with the pure agarose result. Conditions as for Fig. 5.

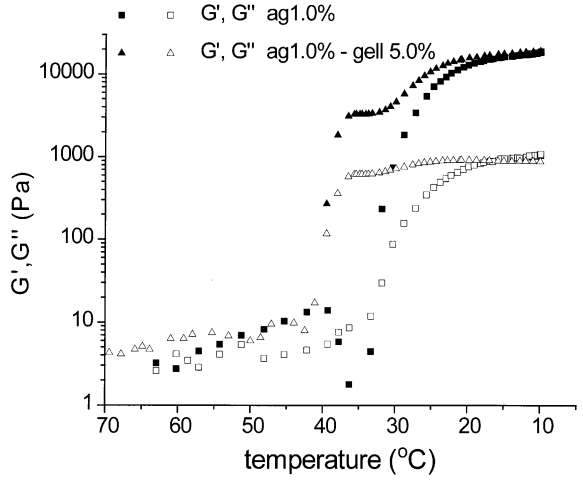

Fig. 7. G' and G'' cure curves for the agarose 1% w/w–gellan 5% w/w system are compared with the pure agarose result. Conditions as for Fig. 5.

to 5% w/w. Results for the pure gellan systems are included. For these higher gellan systems, where gellan gels first, the turbidity-temperature profiles are not unlike those for the pure gellan itself though, overall, there seems to be a systematic turbidity increase for the mixtures even at high temperatures. Some influence of the gelling agarose appears in the data for the 3% gellan mixture but again the final turbidity is not much higher than for the gellan alone. Interestingly, at lower levels of gellan than shown, the pure gellan contribution is found to be small, and independent of temperature, and in this situation the increase in turbidity observed on cooling can be attributed to agarose, the first gelling component.

More quantitative analysis of light scattering from polymer gel networks is difficult to perform with conviction

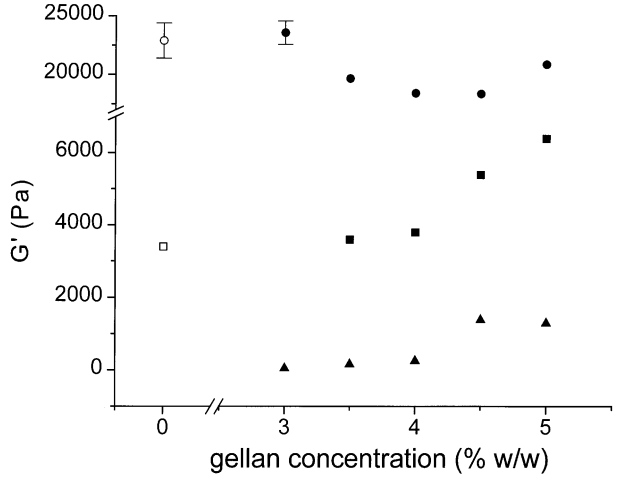

Fig. 8. Summary of plateau G' results for mixtures containing 0.5% w/w (squares) and 1% w/w (circles) agarose and increasing gellan concentrations (typical error bars included). Corresponding results for the pure gellan systems are also shown (triangles). Open symbols indicate pure agarose modulus values. Conditions as in Fig. 5.

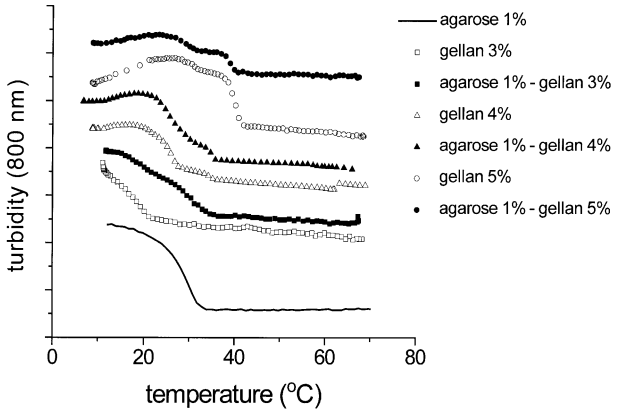

Fig. 9. Turbidity-time data for agarose, gellan and agarose/gellan mixtures for fixed 1% w/w agarose concentration and gellan concentrations in the range 3–5% w/w. Conditions as in Fig. 5.

particularly for the fibrous biopolymer structures involved. What can be concluded with some certainty, however, is that the results presented here seem inconsistent with any form of simple phase separation, as the changes expected would then be much greater, and the final turbidities much harder to relate to those expected for the pure components. Again a picture of almost unperturbed network formation emerges, a picture which finds further support from microscopy.

3.4. Microscopy

Studies of the gelling solutions by both phase contrast and confocal optical microscopy provided no indications whatsoever of phase separation on the distance scales accessible to these techniques. To probe at shorter distances (<1 μm) transmission electron microscopy (TEM) with both conventional and antibody/gold conjugate staining was appealed to.

Micrographs for a 1% agarose and 5% gellan gel appear in Figs. 10 and 11, respectively. Fig. 10 is representative of TEM images commonly obtained for agarose systems, and shows a structure assembled from long connected fibres which are presumably closely bonded bundles of molecular double helices. These fibres are clearly visible, not only through the conventional staining applied, but also by the gold conjugate decoration achieved by antibody labelling (black dots).

The gellan gel micrograph, Fig. 11, on the other hand, shows a denser network structure with smaller pores, and significantly thinner fibre strands. There is the further difference that the gellan network contains quite a number of heterogeneities (dark streaks much thicker than the single fibres) which appear to correspond to sizeable bundles of loosely associated (and aligned) fibres. Since the gellan concentration is quite high in the gel structure displayed, and the effect can be shown to become more pronounced with concentration, this may indicate some tendency towards anisotropic ‘liquid crystal’ phase formation by the

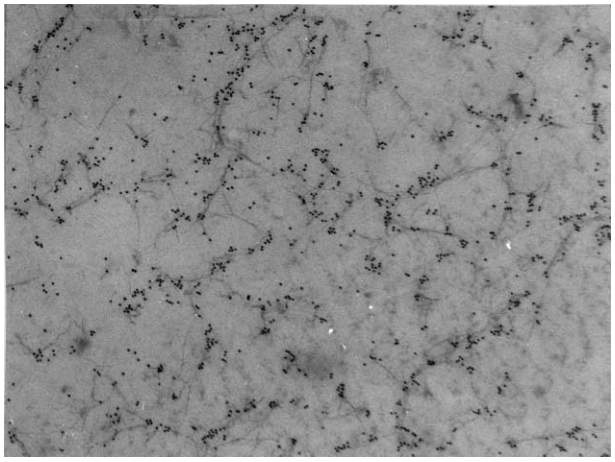

Fig. 10. TEM micrograph of agarose gel (1% w/w). Image maximum dimension is 3 μm. Agarose network strands are highlighted by antibody-gold conjugate labelling (black dots).

ordered gellan. While these anisotropic features are of interest from the point of view of polysaccharide gel microstructure generally, and in the present case help to identify the gellan component in the mixed systems, they do not dominate the structures involved, or (it seems) make major contributions to the mixed gel properties.

Micrographs for one of the mixtures appear in Figs. 12 and 13, i.e. for the 1% agarose/3% gellan system. These present the gel microstructure at two levels of magnification. The high magnification image of Fig. 12 reveals what seems to be a superposition of results for the single biopolymer components with the gellan still showing clumps of aligned fibres, and the agarose network still decorated by

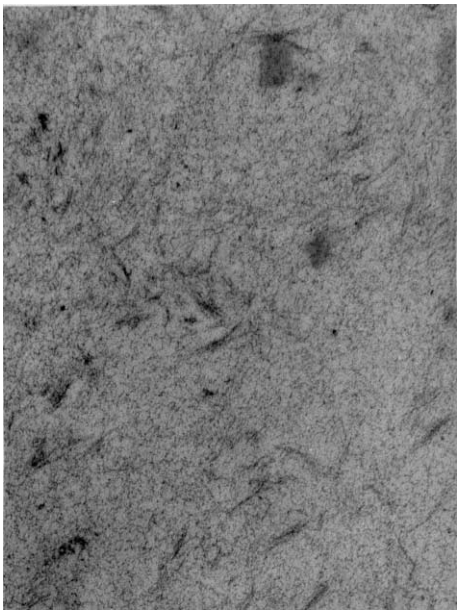

Fig. 11. TEM micrograph of gellan gel (5% w/w). Image maximum dimension corresponds to 3 μm. Darker streaked regions show loosely aligned gellan fibres and possibly indicate anisotropic micro-phase formation.

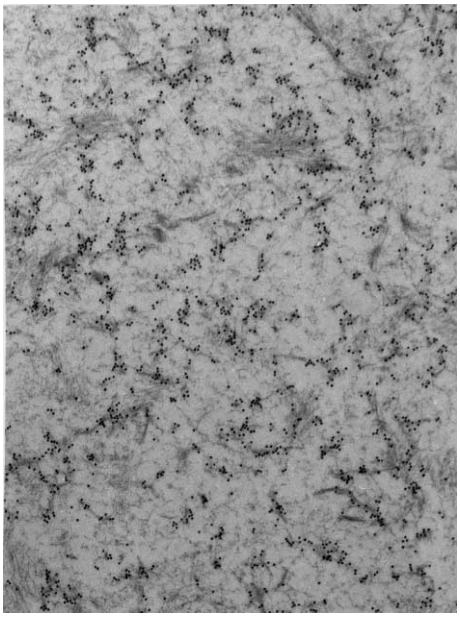

Fig. 12. TEM micrograph of agarose (1% w/w) — gellan (3% w/w) gel. Image maximum dimension corresponds to 3 μm. The structure formed appears to be a superposition of those in Figs. 10 and 11.

the antibody labelling. The low magnification image (Fig. 13) warns, however, that the microstructure is not completely describable in this way. Careful examination of several images showed that, while the structure of Fig. 12 predominates in samples, the agarose content is depleted in certain areas of the gel network (low contrast regions — absence of antibody labelling) leading to a significant level of long-range heterogeneity. In these depleted regions, close examination of the images suggests that there the gellan network is the principal structural component. In addition, there is no suggestion that the gellan suffers a discontinuity on passing to the darker agarose-rich regions, i.e. it appears to extend continuously throughout the gel. There is therefore no evidence of real demixing and phase separation of the components during gelling. Rather, it seems that the agarose, while attempting to build a network within the pores of the pre-formed gellan structure, is unable to distribute itself uniformly. Indeed at the concentrations involved, it may actively concentrate in certain regions of the gellan network and so undergo a form of thermodynamically driven polymer-in-network demixing.

Micrographs obtained for systems at 2% agarose concentration and containing a range of gellan concentrations (not shown) displayed similar structures to the 1% agarose series, but the networks imaged at the lowest agarose level (0.5% w/w) were entirely homogeneous (no depleted regions). These results are in agreement with the idea of the agarose distribution becoming less uniform within the gellan network as both the agarose and gellan concentrations increased. Interestingly, in all cases, in situations involving low (non-gelling) gellan content, and agarose

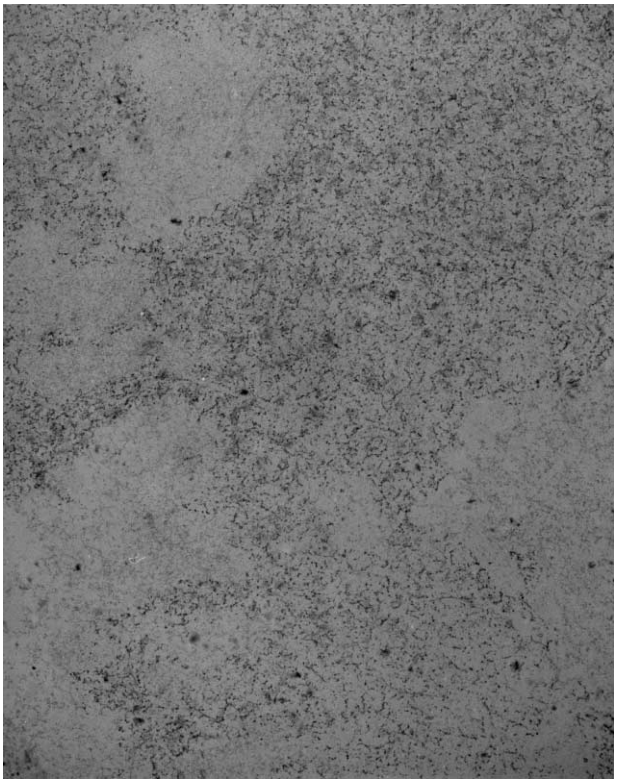

Fig. 13. TEM micrograph of agarose (1% w/w) — gellan (3% w/w) gel. Image maximum dimension corresponds to 24 μm. Darker areas, antibody — gold labelled, indicate long-range heterogeneity in the agarose distribution within the pre-formed gellan network.

gelling first, the networks were also highly uniform. Finally, as mentioned earlier, micrographs for systems made under large variations in cooling rate failed to show substantial changes in microstructure, suggesting that the results described here do not rely heavily on kinetic control.

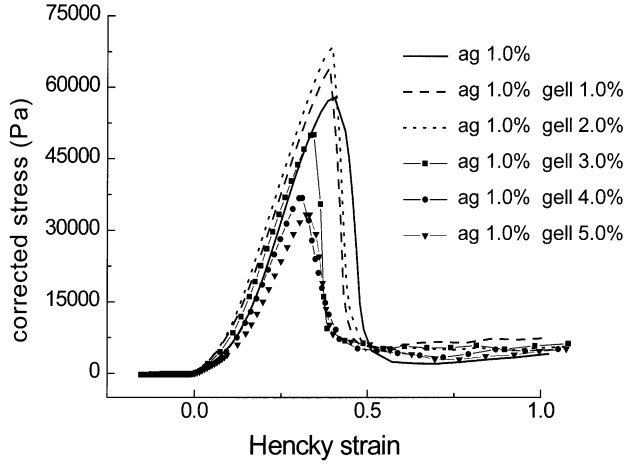

Fig. 14. Typical stress-strain curves for agarose (1.0% w/w) — gellan gels as a function of gellan concentration. Compression rate is 50 mm/min.

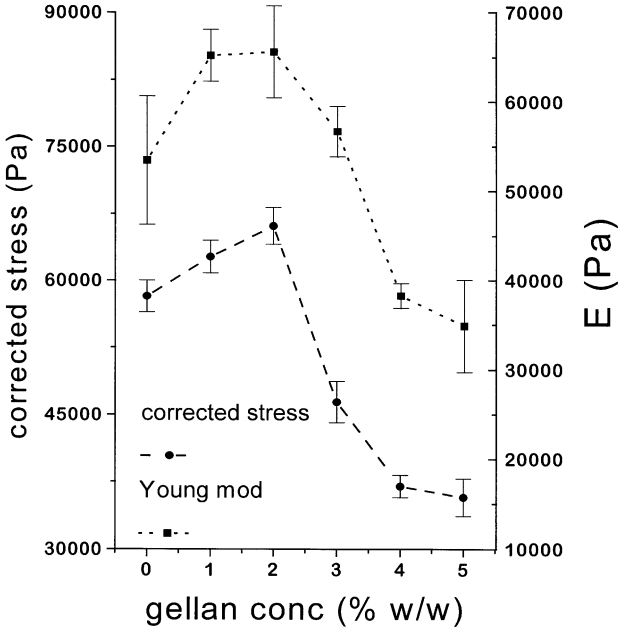

Fig. 15. Stress at fracture and Young's modulus of agarose (1.0% w/w) — gellan gels as a function of gellan concentration. Compression rate is 50 mm/min.

3.5. Compression testing

The large deformation mechanical behaviours of gels are of course of great practical importance, and in the present work the compressive responses of the gels were measured, and compared to results for the individual components. Stress–strain curves for the 1% w/w agarose system, and for its mixtures containing up to 5% gellan, appear in Fig. 14. The pure agarose gel has the largest strain-to-break with the composites becoming more brittle particularly when the gellan content increases beyond 2% w/w. It is at this point, of course, that the gels become gellan dominated (i.e. the gellan gels first).

Young's moduli of compression were estimated from the data as discussed earlier. These appear in Fig. 15 together with values for the stresses-to-break. As for the previously discussed shear moduli, these quantities fall off significantly as the gellan concentration increases beyond 2% w/w, and gellan gels first. The results confirm that the agarose is unable to make its full mechanical contribution to these gellan-dominated systems. This could well be connected to the inhomogeneous network structures that develop in the same circumstances, but other explanations are possible such as inhibition of the agarose helix-helix cross-linking process in the mixed polymer environment. Interestingly, similar large-deformation compressive studies (data not shown) of the more homogeneous 0.5% agarose gel series produced rather different results with the stress and strain-to-break remaining closer to the pure agarose value over the full range of gellan composition.

4. Conclusion

Past studies of charged-uncharged polysaccharide mixtures (Chronakis, Borgstro & Picullel, 1999; Lundin and Hermansson, 1995; Viebke, 1995) have tended to focus on carrageenan–galactomannan systems and have led to the conclusion that there are attractive interactions between the components which lead to 'coupled' networks and a level of 'synergism'. The only previous study of the agarose-gellan combination (Nishinari, Takaya & Watase, 1994) concluded that normal phase separation occurred, though the gellan and agarose samples used were very different from those studied here. In the present work, however, the experimental approaches adopted provide little evidence for coupling or for phase separation. By contrast, they suggest that under the conditions of low ionic strength and purified gellan used, composite gels based on agarose and gellan have an underlying network structure based purely on interpenetration of fibrous assemblies at a level comparable to the pore sizes of the individual networks. The fibres themselves, and their underlying molecular helices, are apparently minimally affected by the mixed character of the systems. There is no evidence of preliminary liquid-liquid demixing in the sol state prior to gelation, and the more subtle effect of microphase separation at the point of gelation also seems absent.

Heterogeneities do arise in some of the final composite structures, however, as revealed by electron microscopy, but these seem to relate more to the non-uniform distribution of agarose within the pores of a pre-formed gellan network, than to mutual segregation of the components. Though other explanations are possible, the anomalies in both the large- and small- deformation mechanical behaviours of the mixtures found at higher polysaccharide concentrations, such as reductions in the expected agarose contributions, may relate closely to this type of inhomogeneity. Certainly, as the agarose concentration falls, moduli become more simply additive, a result that is consistent with the more uniform mixing of the gelling components observed.

In terms of a more quantitative description (modelling) the present system is less than ideal. A model for molecular IPN formation has previously been proposed by one of the present authors (Clark et al., 1999) on the basis of simple additivity of contributions from the component networks, and inclusion of effects arising from mutual influence of the polymers on gelling parameters (e.g. critical concentrations). However this approach requires detailed and accurate modulus data to be available for the pure components under the same gelling conditions, and in the present case this is frustrated by the slippage found in practice for the purified sodium gellan. The generally poor gelling capacity of this polymer at low ionic strength is also a problem, as such composite gel models are optimally tested when the modulus contributions of both components are well matched, i.e. when one component does not massively dominate as was mainly true in the present examples. In practice, we have recently found that commercial gellan, despite its rather complex ion content, is a good candidate for study in mixtures with agarose, as it forms much stronger gels at low concentrations, and these are highly homogeneous. A future publication will describe results for such systems and application of IPN network models to them.

References

Chronakis, I. S., Borgstro, J., & Picullel, L. (1999). Conformation and association of kappa-carrageenan in the presence of locust bean gum in mixed NaI/CsI solutions from rheology and cryo-TEM. *International Journal of Biological Macromolecules*, *25*, 317–328.

Clark, A. H., Eyre, S. C. E., Ferdinando, D. P., & Lagarrigue, S. (1999). Interpenetrating network formation in gellan–maltodextrin gel composites. *Macromolecules*, *32*, 7897–7906.

Clark, A. H. (2000). Direct analysis of experimental tie line data (two polymer–one solvent systems) using Flory–Huggins theory. *Carbohydrate Polymers*, *42*, 337–351.

Flory, P. J. (1953). *Principles of polymer chemistry*, Ithaca, NY: Cornell University Press.

Kasapis, S., Morris, E. R., Norton, I. T., & Clark, A. H. (1993). Phase equilibria and gelation in gelatin/maltodextrin systems 4. Composition dependence of mixed gel moduli. *Carbohydrate Polymers*, *21*, 243–268.

Lundin, L., & Hermansson, A. -M. (1995). Influence of locust bean gum on the rheological behaviour and microstructure of potassium-kappa carrageenan. *Carbohydrate Polymers*, *28*, 91–99.

Lundin, L., Norton, I. T., Foster, T. J., Williams, M. A. K., Hermansson, A. -M., & Bergstrom, E. (2000). Phase separation in mixed biopolymer systems. In P. A. Williams & G. O. Phillips, *Gums and stabilisers for the food industry* (pp. 167–180). Vol. 10. Cambridge, UK: The Royal Society of Chemistry.

Medin, A. S., & Janson, J. -C. (1993). Studies on aqueous polymer two-phase systems containing agarose. *Carbohydrate Polymers*, *22*, 127–136.

Michon, C., Cuvelier, G., Launay, B., & Parker, A. (1996). Viscoelastic behaviour of gelatin/iota-carrageenan mixtures. *Journal of Chemistry and Physics*, *93*, 828–836.

Morris, E. R. (1995). Polysaccharide synergism — more questions than answers. In S. E. Harding, S. E. Hills & J. R. Mitchell, *Biopolymer mixtures* (pp. 247–288). Nottingham, UK: Nottingham University Press.

Morris, V. J. (1986). Multicomponent gels. In G. O. Phillips, D. J. Wedlock & P. A. Williams, *Gums and stabilisers for the food industry*, Vol. 3 (pp. 87–99). London, UK: Elsevier.

Nishinari, K., Takaya, T., & Watase, M. (1994). Rheology and DSC of gellan–agarose mixed gels. In K. Nishinari & E. Doi, *Food hydrocolloids: structures, properties and functions* (pp. 473–476). New York: Plenum Press.

Picullel, L., Bergfeldt, K., & Nilsson, S. (1995). Factors determining phase behaviour of multicomponent polymer systems. In S. E. Harding, S. E. Hills & J. R. Mitchell, *Biopolymer mixtures* (pp. 13–35). Nottingham, UK: Nottingham University Press.

Picullel, L., Iliopoulos, I., Linse, P., Nilsson, S., Turquois, T., Viebke, C., & Zhang, W. (1994). Association and segregation in ternary polymer solutions and gels. In G. O. Phillips, P. A. Williams & D. J. Wedlock, *Gums and stabilisers for the food industry* (pp. 309–322), Vol. 7. Oxford, UK: IRL Press.

Tolstoguzov, V. B. (1995). Some physico-chemical aspects of protein processing in foods. Multicomponent gels. *Food Hydrocolloids*, *9*, 317–332.

Tromp, R. H., Rennie, A. R., & Jones, R. A. L. (1995). Kinetics of simultaneous phase separation and gelation in solutions of dextran and gelatin. *Macromolecules*, *28*, 4129–4138.

Viebke, C. (1995). A light scattering study of carrageenan/galactomannan interactions. *Carbohydrate Polymers*, *28*, 101–105.

Walkenstrom, P., & Hermansson, A. -M. (1996). Fine-stranded mixed gels of whey proteins and gelatin. *Food Hydrocolloids*, *10*, 51–62.